FEBS Letters 506 (2001) 216–220 FEBS 25313

Involvement of protein dynamics in enzyme stability

The case of glucose oxidase

Ahmed Haouz, Jean Marie Glandières, Bernard Alpert*

Laboratoire de Biologie Physico-Chimique, Université Denis Diderot, 2 place Jussieu, 75251 Paris Cedex 05, France

Received 7 June 2001; revised 10 August 2001; accepted 11 August 2001

First published online 21 September 2001

Edited by Judit Ovádi

Abstract Dynamics of glucose oxidase immobilized and in solution were compared through their tryptophan fluorescence spectra, decay times and quenching by acrylamide. Energy barrier for thermal inactivation and melting temperature of both soluble and immobilized enzyme were also measured. Data show that the fluctuation amplitude is at the origin of protein instability.

Key words: Protein dynamics; Glucose oxidase; Immobilized protein; Thermostability; Fluorescence quenching

1. Introduction

Immobilized enzyme often exhibits greater longevity and stability than the enzyme in solution [1]. Indeed, biochemical specific electrodes (biosensors) have the ability to use a single immobilized enzyme aliquot on the transducer to perform thousands of assays [2]. It has been suggested that this behavior could result from a more rigid conformation generated by bonds linking the enzyme to the insoluble carriers [1]. The crystallized protein form also exhibits greater stability than solubilized protein [3].

Glucose oxidase (β-D-glucose:oxygen-1-oxidoreductase, EC 1.1.3.4) from *Aspergillus niger* is a homodimer glycoprotein with a carbohydrate content of 16% (v/v) [4]. The enzyme (160 kDa) contains two tightly bound flavin adenine dinucleotides non-covalently linked [5]. The glucose oxidase catalyzes the oxidation of β-D-glucose by molecular oxygen into δ-gluconolactone which is spontaneously hydrolyzed to gluconic acid [6,7]. The deglycosylated form of the enzyme retains the structure and the activity of the native glycosylated form [8]. However, absence of the sugar envelope reduces its stability. Here too, the longer stability time of the native enzyme is assumed to arise from a higher structural rigidity induced by the carbohydrate–protein coupling [9]. Increased stability of the protein thus appears to be associated with a compactness which would considerably reduce the fluctuation amplitude of its flexible side chains.

We have undertaken comparative studies of the dynamic properties of glucose oxidase, both immobilized and in solution. The dynamic variability was probed by Trp fluorescence quenching studies [10–12]. Thermal inactivation of both soluble and immobilized protein was also carried out to determine the thermodynamic differences in the denaturation process of the stressed and unstressed states.

2. Materials and methods

2.1. Protein preparation

Glucose oxidase from *A. niger* (type X-S) was purchased from Sigma and the gelatin from porcine skin was purchased from Fluka. The protein was immobilized by cross-linkage using glutaraldehyde. For spectroscopic studies, a 40 μl solution of 20 mg/ml of glucose oxidase, 20 μl of gelatin (10% v/v) and 20 μl of 1-ethyl-3-(3-dimethylaminopropyl)carbodiimide 1 M was prepared and diluted to 120 μl of 100 mM sodium phosphate buffer, pH 7.5. 200 μl of this solution was spread homogeneously on a quartz plate and stored at −20°C for 24 h. After defrosting, the plate was rinsed with the phosphate buffer to eliminate any soluble enzyme. For thermal studies of the immobilized form, a 200 μl solution of 20 mg/ml of glucose oxidase, 100 μl of gelatin (10% v/v) and 100 μl of 1-ethyl-3-(3-dimethylamino-propyl)-carbodiimide 1 M was prepared. This solution was diluted in 600 μl of 100 mM sodium phosphate buffer, pH 7.5, and stored at −20°C for 24 h. After defrosting, the gel was pulverized by a polytron, washed and put in suspension in 0.1 M phosphate buffer pH 7.

2.2. Trp fluorescence measurements

Fluorescence spectra were measured with a Perkin-Elmer LS-5B spectrofluorometer. The excitation and emission spectral bandwidths used were 2.5 nm. The enzyme was excited at 295 nm. The optical pathlength was 1 cm for the enzyme in solution (100 mM sodium phosphate buffer) and in a thin layer of gel deposited on the quartz plate. This one was put in the middle of a cuvette containing the phosphate buffer. The excitation beam was at 45° to the plate. In both cases the spectral emission was measured at right angles to the excitation beam. Fluorescence was observed through a Schött cut-off filter passing wavelengths above 310 nm.

Trp fluorescence quenching by acrylamide was carried out for the enzyme in solution and in immobilized form. In both experiments, acrylamide was added to the buffer.

Trp fluorescence intensity decay was measured using the single-photoelectron timing method with synchrotron radiation from the Super-ACO storage ring (LURE, Orsay, France) as a pulsed light source. The bandwidth at half height of ACO pulse (750 ps) was determined by scattered profile given with a depolished quartz plate. Fluorescence decays were observed under magic angle conditions (54.7°) to rule out anisotropic effects. To suppress the scattered ACO pulse, a $CuSO_4$ filter was seated up after the probe. Time resolution was 25 ps per channel with 2048 channels used for decay storage. Analysis of fluorescence decay was performed by the maximum entropy method, using the program FAME and MEMSYS2 subroutines (MEPC, Ltd.) [13]. The fluorescence decay is $f(t) = \Sigma\alpha_i \exp(t/\tau_i)$, where α_i is the pre-exponential factor and τ_i the decay time for the i-th emitting component. The average fluorescence decay time used in the fluorescence quenching treatment was $\langle\tau\rangle = \Sigma f_i \tau_i$ with $f_i = \alpha_i \tau_i / \Sigma\alpha_i \tau_i$.

2.3. Activity assays

Native glucose oxidase (in both soluble and immobilized form) was gradually inactivated by incubation at fixed temperatures (ranging

*Corresponding author. Fax: (33)-1-44276995.
E-mail address: bea@ccr.jussieu.fr (B. Alpert).

PII: S0014-5793(01)02917-9

from 30 to 85°C) for various periods of time (5 min to 1 h), followed by cooling to 0°C to stop the inactivation process. The activity of each sample was assayed at 30°C with an oxygen electrode (Clark electrode) by flowing oxygen consumption, during the reaction. These assays were performed in 2 ml of solution in the presence of an excess of the glucose substrate (100 mM of β-D-glucose = 10 K_m). The reaction rate was expressed as the oxygen uptake per minute and per unit of enzyme concentration [14].

3. Results

3.1. Activity, stability and structural characterization of the immobilized enzyme

Immobilization of glucose oxidase by cross-linkage does not affect its enzymatic activity. Fig. 1 shows the Lineweaver and Burk curves determined on the soluble and immobilized glucose oxidase. The apparent Michaelis constant (K_m) is 6.5 ± 1 mM and 4.5 ± 1 mM for the immobilized and soluble forms, respectively. The maximal turnover rate is V_{max} = 7.2 ± 0.5 μmol of O_2/min for the soluble enzyme and V_{max} = 6.5 ± 0.5 μmol of O_2/min for the immobilized form. The pseudo linearity domain for the D-glucose substrate is the same for both forms (between 10 μM and 2 mM) with a detection limit of 10 μM. In the experimental precision, the small differences in the kinetic parameters can only be due to diffusional effects of the substrate to the heterogeneous phase (protein gel) [15,16].

The thermal denaturation being irreversible, a same interval of heating time (10 min) was chosen to determine the melting points. Fig. 2 shows the residual activity of the glucose oxidase enzyme (soluble and immobilized) which was incubated for 10 min at various temperatures from 30°C to 85°C. Immobilization enhances the enzyme stability since the melting temperature (T_m) increases from 58°C to 76°C.

Protein immobilization does not change the shapes of the Trp fluorescence spectra [17] for the reduced or for the oxidized enzyme (Fig. 3). Absence of change in the emission maxima between the soluble and immobilized enzyme shows that Trp residues remain hindered close to the protein surface [18,19], protected by the carbohydrate envelope. The fluorescence spectra provide evidence that the surrounding microenvironments of the Trp residues are not affected by the immobilization. For the enzyme in solution a Förster coupling mechanism produces a partial energy transfer from seven Trp residues to the flavin [17]. Since the Trp emission does not change with immobilization, there is no alteration in this coupling and no change in the relative Trp-isoalloxazine orientations. Thus, the tertiary organization in the immobilized protein is conserved, whatever the redox state of the flavin.

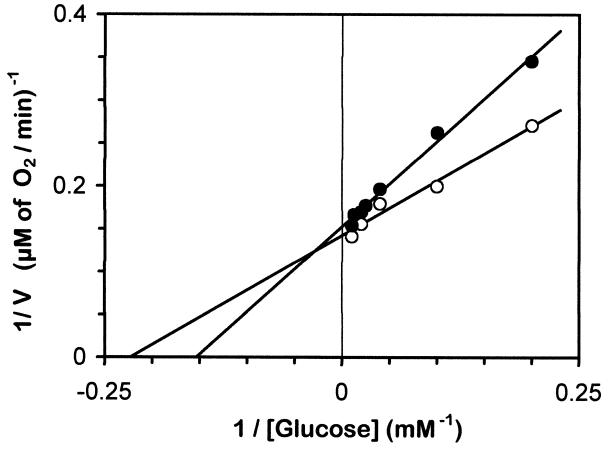

Fig. 1. Immobilization effect on the activity of the glucose oxidase enzyme. (●) Soluble and (○) immobilized forms. The inverse representation $1/V = f(1/[\text{glucose}])$ of the catalytic reaction (at pH 7) gives the two apparent kinetic parameters (K_m and V_{max}) for the soluble and the immobilized forms.

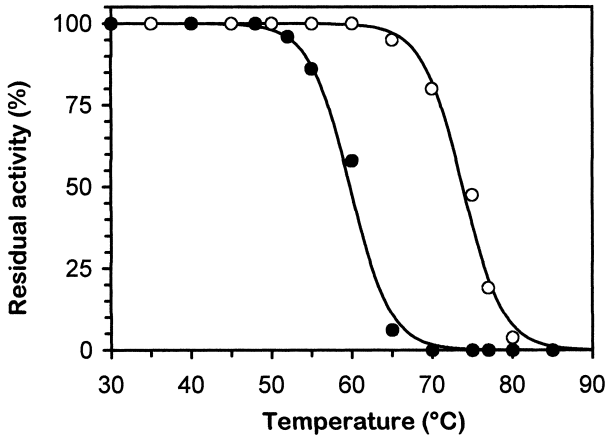

Fig. 2. Loss of the glucose oxidase activity as a function of the heating temperature. (●) Soluble and (○) immobilized forms. Each glucose oxidase sample was heated for 10 min at various temperatures. Residual activity was measured at 30°C with 100 mM glucose (10 K_m).

3.2. Fluctuating tertiary structure of the immobilized enzyme

Free in solution and immobilized in gel, glucose oxidase exhibits the same strong non-exponential Trp fluorescence decay. The change appears only between the various oxidation states of the flavin (Fig. 4). The decays are always the sum of four exponential functions. The enzyme in solution and in gel exhibit the same lifetimes but with small changes in their preexponential factors distribution (Table 1). Protein Trp fluo-

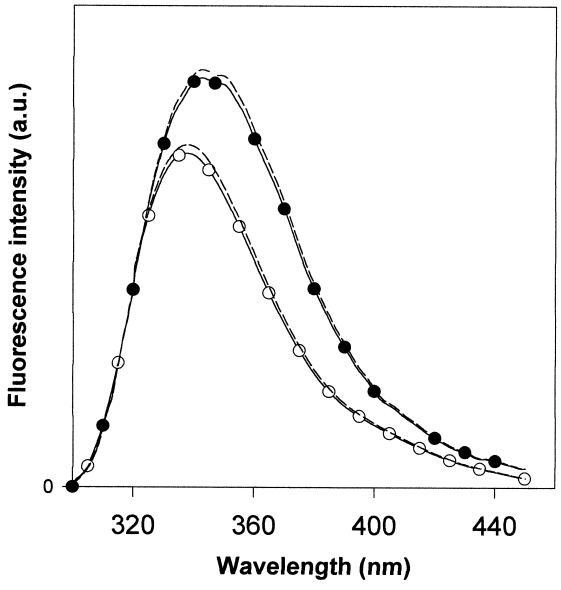

Fig. 3. Trp fluorescence spectra of glucose oxidase in soluble and immobilized forms. (—) Immobilized and (– – –) soluble enzyme. (●) Reduced and (○) oxidized forms. Excitation and emission spectra bandwidths: 2.5 nm. Spectra obtained at 20°C with λ_{exc} = 295 nm.

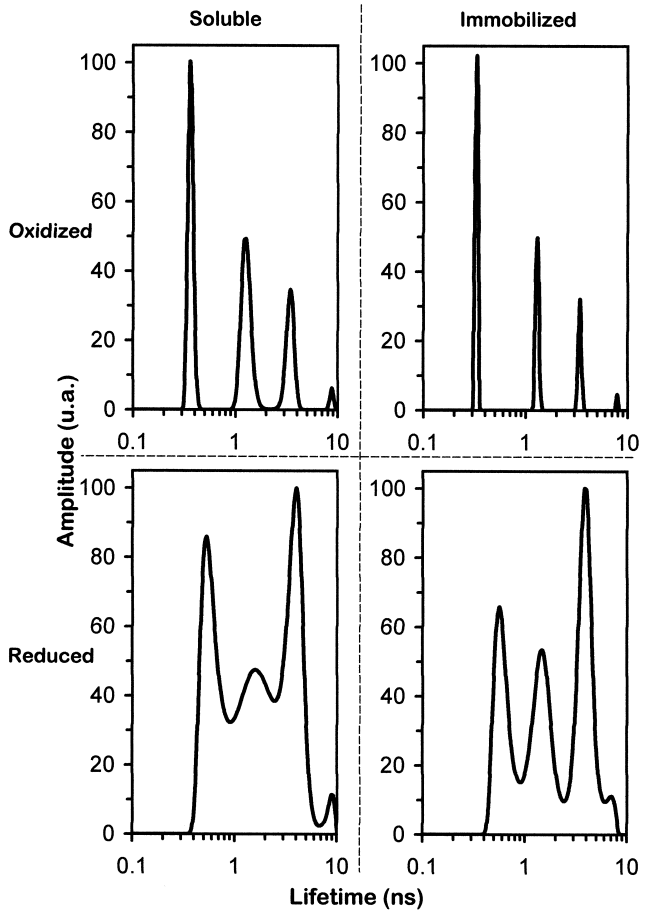

Fig. 4. Trp fluorescence decay times distribution of soluble and immobilized glucose oxidase. The pattern gives the pre-exponential factor α versus the fluorescence decay time τ values in a logarithm scale. Experiments made at 20°C and pH 7.0. $\lambda_{exc} = 300 \pm 1.5$ nm, $\lambda_{em} = 350$ nm with $\Delta\lambda_{em} = 24$ nm. Time resolution: 25 ps/channel. Count: 10^7 photons.

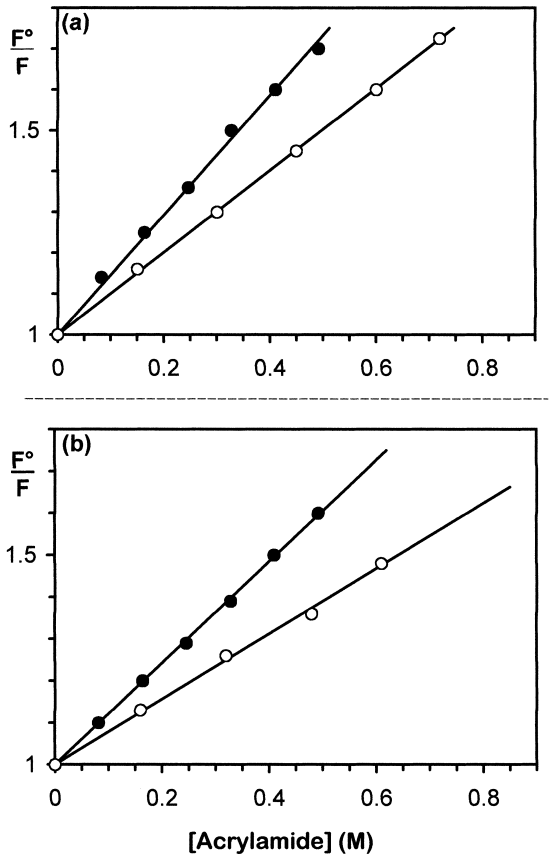

Fig. 5. Stern–Volmer plots of Trp fluorescence quenching of glucose oxidase by acrylamide. Oxidized (a) and reduced (b) forms. Quenching of (●) soluble and (○) immobilized forms at 20°C, pH 7.0.

rescence arises from the Trp excitation energy which is not transferred to the flavin group [17], so the observed decays originate from the emission part of Trp residues in an unfavorable orientation to flavin transfer. Conservation of the lifetime values confirms the unchanged tertiary structure; and the small redistribution of the populations suggests that the rotational freedom of the Trp residues is slightly modified (Table 1). In both media, the Trp orientational relaxation rates are slow compared to the emission lifetimes, and do not differ significantly. These data suggest that the protein fluctuations inside the cross-linked enzyme present similar velocities (frequency distribution) than that in the soluble enzyme, but are differently populated.

3.3. Surface motion of the immobilized enzyme

Surface mobility in regions close to Trp residues was analyzed by Trp fluorescence quenching with acrylamide. Indeed, the average fluorescence lifetime of Trp residues being short, the dynamic quenching represents acrylamide migration near these residues [20,21]. This migration follows the microscopic motions of the surface regions in the vicinity of the Trp residues [19]. Therefore the kinetic constant is an averaged indication of the protein surface mobility. Changes in structural flexibility caused by immobilization of the protein were calcu-

Table 1
Immobilization effect on the Trp fluorescence decay times of glucose oxidase enzyme[a]

Glucose oxidase form	τ^b (ns)	α_i^c (%)	τ^b (ns)	α_i^c (%)	τ^b (ns)	α_i^c (%)	τ^b (ns)	α_i^c (%)	χ	$\langle\tau_0\rangle^d$ (ns)
Soluble oxidized	0.4	41	1.3	36	3.4	21	7.7	2	1.1081	2.9
Immobilized oxidized	0.4	53	1.3	29	3.4	16	7.7	2	1.0344	2.8
Soluble reduced	0.6	32	1.6	30	3.8	36	8.6	2	1.0061	3.4
Immobilized reduced	0.6	28	1.5	30	3.9	40	7.1	2	1.0520	3.4

[a]Excitation wavelength 300 ± 1.5 nm, $\lambda_{em} = 350$ nm ($\Delta\lambda_{em} = 24$ nm). Fluorescence detected at 20°C through a $CuSO_4$ filter. Scattered light is less than 0.1% of the fluorescence signal.
[b]Decay time of each fluorescence component.
[c]Pre-exponential factor of each component.
[d]Average fluorescence decay time (see Section 2). Error: ± 0.05 ns.

lated using the Stern–Volmer representation [22]:

$$\frac{F^0}{F} = 1 + k \times \tau_0 \times Q$$

where F^0/F is the ratio of the Trp fluorescence intensity in the absence and presence of acrylamide, k the kinetic quenching constant, τ_0 the average Trp fluorescence lifetime in absence of quencher, and Q the acrylamide concentration. Fig. 5 and Table 2 show the quenching data for the soluble and the immobilized enzyme.

The observed Trp fluorescence quenching suggests that the immobilized enzyme exhibits an internal self-friction greater than that of the protein in solution. This result is in agreement with the fluorescence lifetime observation which showed a narrower distribution in the times of Trp emission for the immobilized enzyme (Fig. 4). Without perturbing the structure, the cross-linkage in a lattice shortens the length of the flexible chains and the magnitude of their fluctuations. Cross-linkage would restrict the access of acrylamide and thus influences the extent of the Trp fluorescence quenching. Indeed such conditions could exclude some parts of the protein to acrylamide access and abolish acrylamide encounter with particular Trp residues. In fact, the Stern–Volmer quenching curves are linear indicating that all the tryptophan residues stay accessible. Thus, the overall protein fluctuations are present in the gel but their amplitudes are decreased. This result indicates that the structure and the dynamics of the immobilized enzyme are largely intact; only its rigidity is changed.

3.4. Energy barrier for thermal inactivation of the immobilized protein

Active glucose oxidase enzyme, in solution and immobilized, was progressively and irreversibly inactivated by heat, at various temperatures. The remaining enzyme activity (V_{max}) after different periods of heating time (t) permits determination of the kinetics constant (k_{inact}) of the thermal inactivation [1].

$$\ln\frac{(V_{max})_t}{(Vmax)_0} = -k_{inact}(t)$$

The kinetics of inactivation of the immobilized enzyme indicate a first order reaction like soluble enzyme (Fig. 6, top). The activation energy (E_a) of enzyme inactivation for each protein environment can be determined by:

$$\ln(k_{inact}) = -\frac{E_a}{RT} + cte$$

Table 2
Immobilization effect on Trp fluorescence quenching of glucose oxidase by acrylamide at 20°C

Glucose oxidase form	K^a (M^{-1})	$\langle\tau_0\rangle^b$ (ns)	k^c (10^8 M^{-1} s^{-1})
Soluble oxidized	1.4	2.9	4.8
Immobilized oxidized	1.0	2.8	3.6
Soluble reduced	1.2	3.4	3.5
Immobilized reduced	0.8	3.4	2.3

[a] K = Stern–Volmer quenching constant. Precision: ±0.05 M^{-1}.
[b] $\langle\tau_0\rangle$: average fluorescence decay time in the absence of quencher.
[c] k: bimolecular collisional kinetic constant. Precision: $\pm 0.25\times10^8$ M^{-1} s^{-1}.

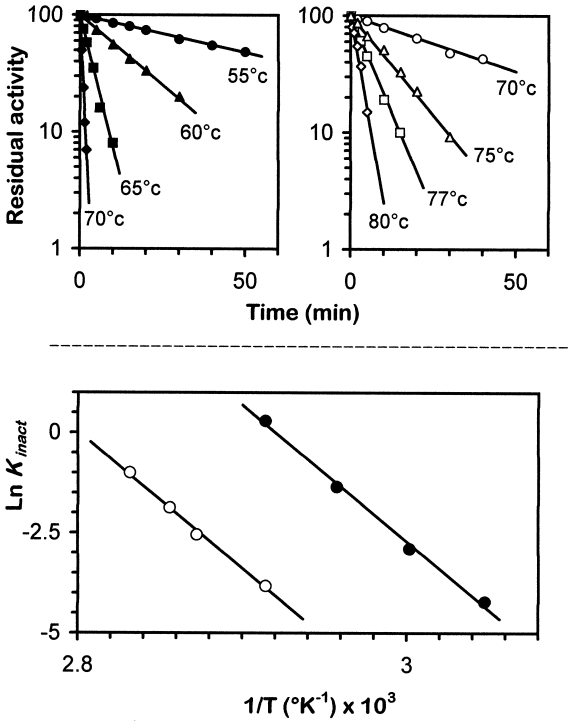

Fig. 6. Thermoinactivation of soluble and immobilized glucose oxidase. Top: kinetics of the thermoinactivation in semi-logarithmic representations; left: soluble form, right: immobilized form. After each incubation time, sample was cooled to 0°C and its activity was measured at 30°C with 100 mM of glucose (10 K_m). Bottom: Arrhenius plots of glucose oxidase inactivation. (●) Soluble and (○) immobilized enzyme. Activation energy of the enzyme inactivation = 70 ± 3 kcal/mol.

where R (2 kcal/K/mol) is the gas constant and T the temperature in Kelvin.

The Arrhenius plots for soluble and immobilized oxidized enzyme are also shown in Fig. 6 (bottom). Both conditions give the same energy barrier E_a = 70 kcal/mol. This shows that thermal inactivation leads essentially to the same energetic disruption in the soluble and immobilized states. Moreover, the curves show that the positive activation entropy for the immobilized protein is smaller than for the soluble form. Thus, the stabilizing effect of the gel comes from a smaller increase in disorder upon going to the transition state. Therefore, soluble and immobilized enzyme evolve to the denatured state with their own statistical factor ($\exp(\Delta S^*/R)$) which would depend both on the conformers distribution and their dynamics. Thus, the different environment conditions do not modify the conformational transition state, they only change the thermodynamic pathway to break the native interactions.

4. Discussion

We have shown that the energy barrier for glucose oxidase inactivation is the same in solution and in the immobilized protein, thus indicating that protein denaturation occurs by the same conformational transition state in both forms. The gel confines the protein to a restricted space. Possibly the protein moiety would be squeezed but its configuration remains intact. The melting temperature (T_m) is, however, higher for the immobilized protein. This higher value of T_m may be ascribed to the kinetic energy of chain motion which dis-

rupts the native protein organization during denaturation. Indeed, T_m should depend on the relation linking protein structure to internal dynamics during the thermodenaturation process. The activation energy (E_a) is the energy required to convert the protein structure between the native form and the transition state of the inactivated conformation. T_m reflects the kinetic energy required by the chain motions to reach the upper amplitude limit which permits this conformational disruption. Therefore, thermodenaturation of the enzyme is determined by two independent parameters: the energy barrier and the melting temperature. Immobilization does not affect the protein structure but it decreases the conformers distribution. The protein dynamics are highly restrained and fluctuation amplitudes are lower. To obtain a larger amplitude of protein motions in gel, the temperature must be higher than that required to destabilize and destroy the protein organization in solution. Then the stabilization induced by immobilization involves the restricted motions of the protein matrix. As a result this enzyme stability is partly determined by the magnitude of the protein motions. So, T_m can be used as an index for the stability of the protein in different environments: the higher T_m, the greater the protection from the thermal deterioration.

T_m can also be regarded as the lowest temperature which can generate a thermal gradient permitting the energetic compensation against the stabilizing forces of the protein. It reflects the elastic limit from the protein surface flexibility. Then, T_m appears as a parameter of the hydrodynamic stability [23]. It is the breaking point of the competition between two opposite energy generators: internal energy and kinetic energy. Several methods have been used to increase protein stability based on structural hierarchies in proteins with significant activation barriers [1]. In a recent review, Freire has summarized the thermodynamic linkage between protein stability, structure and function [24]. The present work shows that the forces which maintain biological structure and those which generate protein fluctuations are both implicated in the protein stability. Thus, the protein dynamics are an important aspect which should be considered to interpret the different protein transition states. The extent of the dynamic implication in the protein stability depends on the fluctuations amplitude. The larger the amplitude, the greater the protein instability. So the favoring conditions for protein stability are closely related to the two processes: one structural and the other dynamic. In the glucose oxidase case the high content of α-helix supporting the anti-parallel β-sheet [7] would create sufficient constraints to limit the extent of the motions near the protein surface and be responsible for the particular longevity of this enzyme.

Acknowledgements: We are very much indebted to Dr. Merola Fabienne for his help, and to the staff at LURE (Orsay, France) for technical assistance at the synchrotron.

References

[1] Mozhaev, V.V. (1993) Trends Biotechnol. 11, 88–95.
[2] Luong, J.H.T., Bouvrette, P. and Male, B. (1997) Trends Biotechnol. 15, 369–377.
[3] Shenoy, B., Wang, Y., Shan, W. and Margolin, A.L. (2001) Biotechnol. Bioeng. 73, 358–369.
[4] Hayashi, S. and Nakamura, S. (1981) Biochim. Biophys. Acta 657, 40–51.
[5] Pasur, J.H. and Kleppe, K. (1964) Biochemistry 3, 578–583.
[6] Bentley, R. (1963) Enzymes 7, 567–587.
[7] Hecht, H.J., Kalisz, H.M., Hendle, J., Schmid, R.D. and Schomburg, D. (1993) J. Mol. Biol. 229, 153–172.
[8] Kalisz, H.M., Hecht, H.J., Schomburg, D., Schmid, R.D. and Schomburg, D. (1991) Biochim. Biophys. Acta 1080, 138–142.
[9] Nakamura, S., Hayashi, S. and Koga, K. (1976) Biochim. Biophys. Acta 445, 294–308.
[10] Lakowicz, J.R. and Weber, G. (1973) Biochemistry 12, 4171–4179.
[11] Eftink, M.R. and Ghiron, C.A. (1975) Proc. Natl. Acad. Sci. USA 72, 3290–3294.
[12] Eftink, M.R. and Ghiron, C.A. (1981) Anal. Biochem. 114, 199–227.
[13] Livesay, A.K. and Brochon, J.C. (1987) Biophys. J. 52, 693–706.
[14] Haouz, A., Geloso, A. and Burstein, C. (1994) Microb. Technol. 16, 292–297.
[15] Bodálo, A., Gómez, J.L., Gómez, E., Bastida, J., Iborra, J.L. and Manjón, A. (1986) Enzyme Microb. Technol. 8, 433–438.
[16] Chaplin, M.F. and Bucke, C. (1990) Enzyme Technology, Cambridge University Press, Cambridge.
[17] Haouz, A., Twist, C., Zentz, C., de Kersabiac, A.M., Pin, S. and Alpert, B. (1998) Chem. Phys. Lett. 294, 197–203.
[18] Burstein, E.A., Vedenkiva, N.S. and Ikova, M.N. (1973) Photochem. Photobiol. 18, 263–279.
[19] Haouz, A., Twist, C., Zentz, C. and Alpert, B. (1998) Eur. Biophys. J. 27, 19–25.
[20] Gratton, E., Jameson, D.M., Weber, G. and Alpert, B. (1984) Biophys. J. 45, 789–794.
[21] Albani, J. and Alpert, B. (1987) Eur. J. Biochem. 162, 175–178.
[22] Stern, O. and Volmer, M. (1919) Phys. Z. 20, 183–193.
[23] Chandrasekhar, C. (1961) Hydrodynamic and Hydromagnetic Stability, Clarendon Press, Oxford.
[24] Freire, E. (2001) Methods Mol. Biol. 168, 37–68.